IEEE Access
Multidisciplinary | Rapid Review | Open Access Journal

Received August 4, 2019, accepted August 17, 2019, date of publication August 23, 2019, date of current version September 6, 2019.

Digital Object Identifier 10.1109/ACCESS.2019.2937193

Classification of Power Quality Disturbances Using Wigner-Ville Distribution and Deep Convolutional Neural Networks

KEWEI CAI[1], WENPING CAO[2], (Senior Member, IEEE), LASSI AARNIOVUORI[3], (Member, IEEE), HONGSHUAI PANG[1], YUANSHAN LIN[1], AND GUOFENG LI[4]

[1]College of Information Engineering, Dalian Ocean University, Dalian 116023, China
[2]College of Electrical and Power Engineering, Taiyuan University of Technology, Taiyuan 030024, China
[3]LUT School of Energy Systems, LUT University, 53851 Lappeenranta, Finland
[4]School of Electrical Engineering, Dalian University of Technology, Dalian 116024, China

Corresponding author: Wenping Cao (caowenping@hotmail.com)

This work was supported by the Foundation of Liaoning Province Education Administration (grant number L201609), the Doctoral Start-up Foundation of Liaoning Province (grant number 20170520191) and National Natural Science Foundation of China (grant number 61603067).

ABSTRACT This paper proposes a hybrid approach combining Wigner-Ville distribution (WVD) with convolutional neural network (CNN) for power quality disturbance (PQD) classification. Firstly, a WVD technique is developed to transfer a 1D voltage disturbance signal into a 2D image file, followed by a CNN model developed for the image classification. Then, the feature maps are extracted automatically from the image file and different patterns are extracted from variables on CNN. A set of synthetic signals, as well as real-world measurement data, are used to test the proposed method. The high classification accuracy of test results is achieved to confirm the effectiveness of the proposed method. Furthermore, the model is simplified and optimized by visualizing the output of convolutional layers. On this basis, one visualizing technique called the class activation map (CAM) is used to identify the location and shape of ''hotspots (PQDs)''. The effect of incorrect classification of the model is analyzed with the CAM. Therefore, the proposed method is proved to have the capability of providing necessary and accurate information for PQDs, which will then be used to determine the subsequent PQ remedy actions accordingly.

INDEX TERMS Classification, convolutional neural network (CNN), deep learning, power quality disturbances, power systems, Wigner-Ville distribution (WVD).

I. INTRODUCTION

Nowadays, power quality (PQ) has been a significant issue in the power system, owing to the increasing penetration of renewable energy into the smart grid network and uptake of electric vehicles (EVs) [1], [2], impacting on the power system stability. In theory, PQ refers to multifarious electromagnetic phenomena that deviate voltage and current from ideal waveforms, which are known as PQ disturbances (PQDs). These disturbances greatly affect the safe and economical operation of the smart grid networks and decrease the lifetime and performance of electrical equipment connected to the system. In order to minimize the impact of these PQDs on the network, an accurate classification of PQDs is critically important. Therefore, an intelligent and automated technique for PQD classification is an urgent need.

According to the international standards such as EN 50160 [3], IEC 61000 [4], and IEEE-1159 [5], PQDs include voltage sags, swells, interruptions, oscillations, flickers, and harmonics. Conventionally, the PQD identification and disturbance classification are carried out in two steps: feature extraction and classification. Signal processing techniques, such as Fourier transform (FT) [6], short-time Fourier transform (STFT) [7], [8], wavelet transform (WT) [9]–[11], S-transform (ST) [12], [13], Wigner-Ville distribution (WVD) [14], empirical mode decomposition (EMD) [15]–[17], independent component analysis (ICA) [18], and variational mode decomposition (VMD)

The associate editor coordinating the review of this article and approving it for publication was Hui Liu.

[19]–[21] are all found in use for feature extraction. FT is simple to implement but it is unsuitable for non-stationary disturbances due to its lack of time-frequency localization capability. STFT analyzes non-stationary signals by a sliding window and obtains the time and frequency information. However, this method is constrained by the size of the sliding window. WT could enhance the time-frequency resolution for disturbance analysis, but it is sensitive to noise. The ST generalizes the STFT, extends WT and overcomes some of the WT disadvantages. Therefore, the ST is superior to the FT, STFT, and WT techniques, especially for the noise-rich systems. Nevertheless, the widespread application of ST is limited by its computational complexity. In recent years, the WVD method has received considerable attention as an analysis tool for non-stationary signals due to its high time-frequency resolution and excellent performance in the presence of noise. EMD is an adaptive time-frequency method for analyzing non-stationary signals and can decompose signal into a finite number of intrinsic mode functions (IMFs). However, it has some inherent drawbacks, e.g., a mode mixing and boundary effects (leading to false IMF decomposition). An EMD-ICA technique was proposed to overcome these issues. This technique is effective to eliminate the mode mixing but suffers from the absence of the amplitude information because of the added ICA. VMD decomposes a multimode signal into a finite number of band-limited IMFs. Compared with EMD-based methods, The VMD is a more robust method to noise and sampling errors as it can generalize a classical Wiener filter into multiple, and adaptive bands [22], [23]. The above signal processing methods are often used to extract feature from different types of PQDs.

After a feature is extracted, the disturbance classification is conducted by a specific rule. In the literature, the typical disturbance classification methods include support vector machine (SVM) [24], [25], decision tree (DT) [26], [27], artificial neural network (ANN) [28], and probabilistic neural network (PNN) [29], [30]. Among these, the SVM is the most widely used technique, which is based on small number of sample and structural risks minimized. Similarly, DT is a decision support-making tool in a tree-like graph that is used to describe the relationship of different features, and to make classification; it has also been used to identify PQDs. Nevertheless, the SVM and DT methods give rise to cumulative errors in the process of the iterative classification of all disturbances. To overcome this, ANN-based classifiers are widely used through an expeditious learning process. This process has no iterations or cumulative errors. PNN is derived from the Bayesian network and the kernel fisher discriminant analysis algorithm. It is faster and more accurate than ANN.

The existing methods composed of feature extraction and classification techniques have been proved to be effective, but have three limitations: 1) The features extracted from PQD signals are hand-crafted. Different types and quantities of the features have differing influence on the classification results. For the PQDs classification task. In current research, the process of feature extraction relies heavily on hand-crafted, various features with different number and type. For example, relative mode energy ratio (RMER), mode's center frequency, number of zero-crossings and instantaneous amplitude (IA) are used in [20]; mean, variance and kurtosis are used in [21]. The accuracy of the classifier is open to interpret if key features were missed out; 2) The feature extraction and classification are two independent processes but the parameters of classification methods could be optimized as per PQD data. Nevertheless, the parameters of feature extraction methods are fixed once the feature extraction is completed. Therefore, the features of disturbance signals can not be updated afterwards. The fixed features would limit the accuracy of the classification results; 3) These methods are shallow learning methods in their nature. Their performance is below deep-learning methods because the latter have deep layer topology and big data support [31], [32]. For this reason, a new deep learning technique for PQD classification is proposed in this paper to automatically extract features, optimize both parameters of feature extraction and classification methods, and simultaneously analyze all the nonlinear, non-stationary synthetic and real-world signals without a need for human intervention. In the literature, the convolutional neural networks (CNNs) have become an emerging and popular technique in deep learning technologies [32]. The CNN is a biologically inspired feedforward ANN that presents a simple model for the mammalian visual cortex. It has been widely used in the visual field, such as image recognition [33], [34] and video classification [35]. They have been applied to a wide range of tasks related to signal, image and information processing in the artificial intelligence (AI) domain. Deep learning algorithms are capable of learning optimal features from raw input data automatically through using multiple levels of abstraction and representation of the signal, and image data. Several methodologies based on deep learning have been used to identify the types of PQDs. The estimation of voltage sags in sparsely monitored power systems by using CNN model, is reported in [36]. The CNN combining with a long short term memory (LSTM) method is used for PQDs classification in [37]. The PQDs are estimated based on a deep belief network (DBF) in [38]. Although these methods obtain satisfactory PQD results, they struggle with the separation analysis of multiple PQDs.

In this paper, a novel method combining WVD with CNN for PQD classification is proposed to utilize the key features of existing methods. Firstly, the WVD method is used to convert a 1D raw data of PQDs into a 2D image file. Then, a CNN based model is developed to classify the images for PQDs recognition, which will improve the quality of classification. Furthermore, the model network optimization is also achieved through CNN visualization techniques [39], [40]. The performance of the proposed method is tested by nine types of synthetic PQDs as well as real-world measurements from the IEEE Working Group on Power Quality Data Analytics.

The remainder of this paper is organized as follows: Section II presents the proposed algorithms based on the

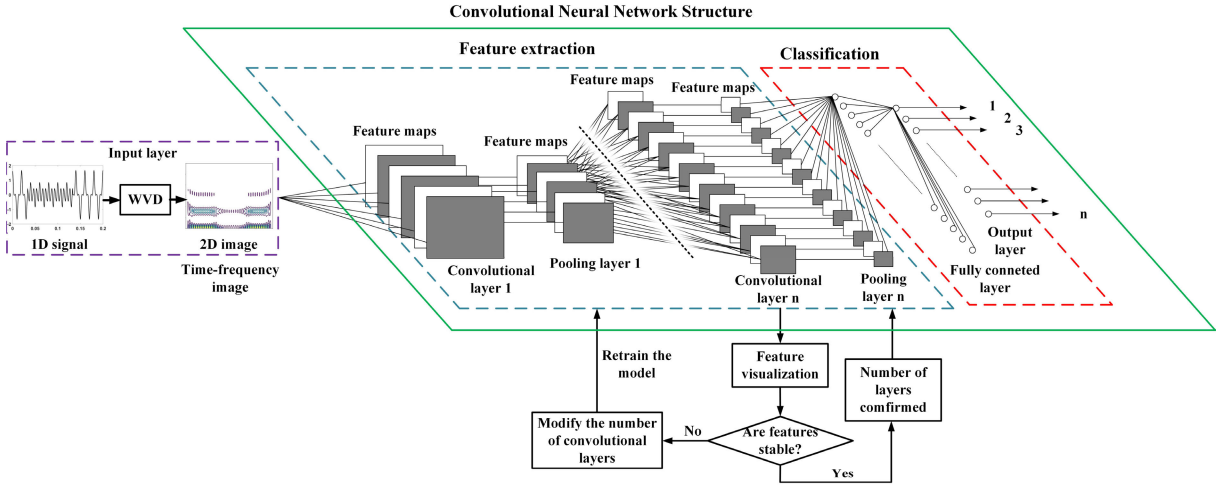

FIGURE 1. The main framework of the proposed method.

WVD and CNN models. Section III introduces the implementation of the WVD-CNN method for PQDs classification. Section IV presents the discussion and classification of the results using different types of synthetic cases and real-world data. Finally, the concluding remarks are drawn in Section V.

II. DESCRIPTION OF METHODOLOGY

The framework of the proposed method is illustrated in Fig. 1. Firstly, the sequence voltage data are transformed into the time-frequency domain images by using WVD technique. Then, the images are the inputs to a CNN model to classify the types of disturbances. In the CNN model, the feature visualization method is taken to optimize the construction of the model.

A. WIGNER-VILLE DISTRIBUTION (WVD)

WVD can provide quantitative information of the signal energy distribution in time-frequency domain. Mathematically, the WVD representation is defined by:

$$WVD\,(t,f) = \int_{-\infty}^{\infty} s(t+\frac{\tau}{2})s^*(t-\frac{\tau}{2})e^{-j2\pi}\,d\tau \qquad (1)$$

where t is the sampling time, f is the frequency, $s(t)$ is the time series signal, $s^*(t)$ is the conjugate variable of $s(t)$, and τ is the delay variable. In the frequency domain, the definition of WVD can be illustrated as:

$$WVD_{fre}\,(t,f) = \int_{-\infty}^{\infty} S(f+\frac{\varphi}{2})S^*(f-\frac{\varphi}{2})e^{j2\pi}\,d\varphi \qquad (2)$$

where S(t) is the Fourier transform of $s(t)$, φ is the delay variable in the frequency domain.

The purpose for using the Wigner function is to reduce the spectral density function of the time for time series signals, so as to achieve the non-stationary autocorrelation. Therefore, a time series voltage signal can be expressed in the time-frequency domain and transferred into a time-frequency image. Moreover, the different types of disturbance signals can be transferred into different WVD images. Then, the 2D image is input to the CNN model for PQD classification. Hence, the PQDs can be identified in a graphical perspective. This is easier than a 1D approach.

In essence, the two definitions of WVD in (1) and (2) are equivalent. However, the definition in the frequency domain requires a knowledge of the Fourier transform of the original signal, which is more complex to implement. In this work, the time domain definition of WVD is used.

B. CONVOLUTIONAL NEURAL NETWORK (CNN)

Typically, a fundamental framework of CNN model consists of an input layer, convolutional layers, pooling layers, fully-connected layers, and an output layer.

The convolutional layer is the core part of CNN. It uses the mathematical 2D convolution operation to transfer low-level local features into high-level global features. Herein, the convolution operator is used to extract image features by preserving the spatial relationship between pixels of the image matrix. It is performed on the input image data with a kernel to produce a feature map. In this paper, a 3×3 convolution kernel is developed. The convolution operation is implemented by:

$$c_{ij}^k = \sum\nolimits_{m=0}^{2}\sum\nolimits_{n=0}^{2} w_{m,n}x_{i+m,j+n} + b^k \qquad (3)$$

where w is the weight of the kernel, x is the input data of this layer, b is the bias term, c is the result of convolution operation, k is the number of kernels, i, j and m, n are the location labels of the original image and convolution kernel matrices, respectively.

A weight sharing technique is adopted to share neurons in different layers so as to help the process of feedforward and backpropagation (BP) [41]. By doing so, the number of parameters under consideration is effectively reduced. Through the convolution layer, the hidden invariant features in data are extracted automatically. The pooling layer

TABLE 1. Expressions of simulated PQ disturbances.

PQ Disturbance	Label	Numerical model	Parameters
Sag	Sag	$v(t) = (1 - \alpha(u(t-t_1) - u(t-t_2)))\sin\omega t$	$0.1 \le \alpha \le 0.9, T \le t_2 - t_1 \le 9T$
Swell	Swell	$v(t) = (1 + \alpha(u(t-t_1) - u(t-t_2)))\sin\omega t$	$0.1 \le \alpha \le 0.8, T \le t_2 - t_1 \le 9T$
Interruption	Inter	$v(t) = (1 - \alpha(u(t-t_1) - u(t-t_2)))\sin\omega t$	$0.9 \le \alpha \le 1, T \le t_2 - t_1 \le 9T$
Flicker	Flicker	$v(t) = (1 + \alpha_f \sin(\beta\omega t))\sin\omega t$	$0.1 \le \alpha_f \le 0.2, 5 \le \beta \le 20\text{Hz}$
Harmonic	Har	$v(t) = \alpha_1\sin\omega t + \alpha_3\sin 3\omega t + \alpha_5\sin 5\omega t$	$0.05 \le \alpha_3, \alpha_5 \le 0.15,\ \sum \alpha_i^2 = 1$
Oscillatory Transient	Osc	$v(t) = \sin\omega t + \alpha e^{-\frac{(t-t_1)}{\tau_0}} \sin\omega_n(t-t_1) \times \{u(t_2) - u(t_1)\}$	$0.1 \le \alpha \le 0.8,$ $0.5T \le t_2 - t_1 \le 3T,$ $8ms \le \tau_0 \le 40\text{ms},$ $300 \le f_n \le 900\text{Hz}$
Sag & Harmonic	Sag & Har	$v(t) = \left(1 - \alpha\left(u(t-t_1) - u(t-t_2)\right)\right) \times (\alpha_1\sin\omega t + \alpha_3\sin 3\omega t + \alpha_5\sin 5\omega t)$	$0.1 \le \alpha \le 0.9, T \le t_2 - t_1 \le 9T$ $0.05 \le \alpha_3, \alpha_5 \le 0.15,\ \sum \alpha_i^2 = 1$
Interruption & Harmonic	Inter & Har	$v(t) = \left(1 - \alpha\left(u(t-t_1) - u(t-t_2)\right)\right) \times (\alpha_1\sin\omega t + \alpha_3\sin 3\omega t + \alpha_5\sin 5\omega t)$	$0.9 \le \alpha \le 1, T \le t_2 - t_1 \le 9T$ $0.05 \le \alpha_3, \alpha_5 \le 0.15,\ \sum \alpha_i^2 = 1$
Swell & Harmonic	Swell & Har	$v(t) = \left(1 + \alpha\left(u(t-t_1) - u(t-t_2)\right)\right) \times (\alpha_1\sin\omega t + \alpha_3\sin 3\omega t + \alpha_5\sin 5\omega t)$	$0.1 \le \alpha \le 0.8, T \le t_2 - t_1 \le 9T$ $0.05 \le \alpha_3, \alpha_5 \le 0.15,\ \sum \alpha_i^2 = 1$

implements non-linear down-sampling after the convolution layer through a max-pooling (or average-pooling) method. The output of the convolution layer is divided into a set of non-overlapping rectangles, generating maximum (or average) of each sub-region. This layer is employed to reduce the spatial size of the representation progressively, and decrease the number of parameters so as to reduce the overfitting issue. Finally, a fully connected layer is created to combine all the feature maps with a final classification vector. It is fed into the output layer.

III. THE PROPOSED PQD CLASSIFICATION METHOD

Based on the above mentioned WVD and CNN algorithms, a new PQD classification method is developed.

A. THE EXPRESSIONS OF PQD SIGNAL

In this work, nine types of single and mixed voltage disturbance signals are synthesized in MATLAB according to the IEEE-1159 [5]. The amplitudes of the synthetic signals are normalized to 1 p.u. The fundamental frequency is set at 50 Hz, and the sampling frequency of synthetic signal is 6.4kHz. There are 10 cycles in every synthetic signal and one cycle contains 128 sampling points. The expressions of these PQDs are shown in Table 1. The synthetic disturbance signals have the signal-to-noise ratio of 10-40dB, as the amplitude of disturbance signals is chosen randomly allocated. The original signals and transferred 2D images are illustrated in Fig. 2. Each image has 200×200 pixels as the input of CNN model.

B. THE MODEL OF THE PROPOSED METHOD

The proposed method has an input layer, three convolutional layers, three max-pooling layers, a fully connecting layer, and an output layer, as illustrated in Fig. 3. The number of convolutional kernels in the three different convolutional layers are 32, 64 and 64, respectively. The features of the PQDs images are extracted by using the convolution operator, which preserves the spatial characteristics of the image matrix. In particular, a kernel slides over an input image by

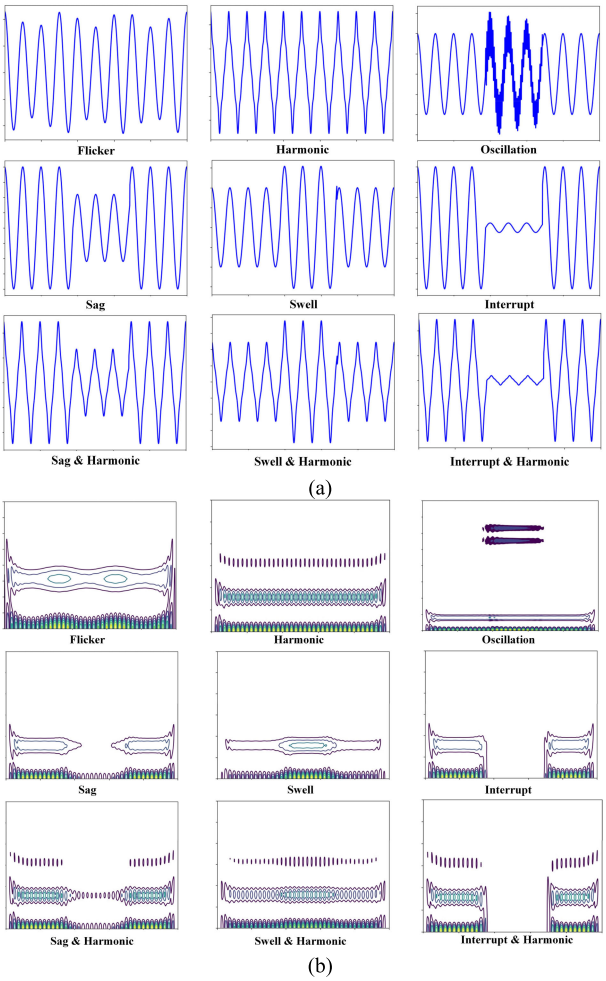

FIGURE 2. The original PQD signals and the 2D images transferred by using the WVD method, (a) original signals, (b) 2D images.

using (3) to produce a feature map and the stride size of the sliding is 1. To guarantee the process of feature extraction, the zero-padding method is used to preserve the information of the input signal. In the process of feature extraction,

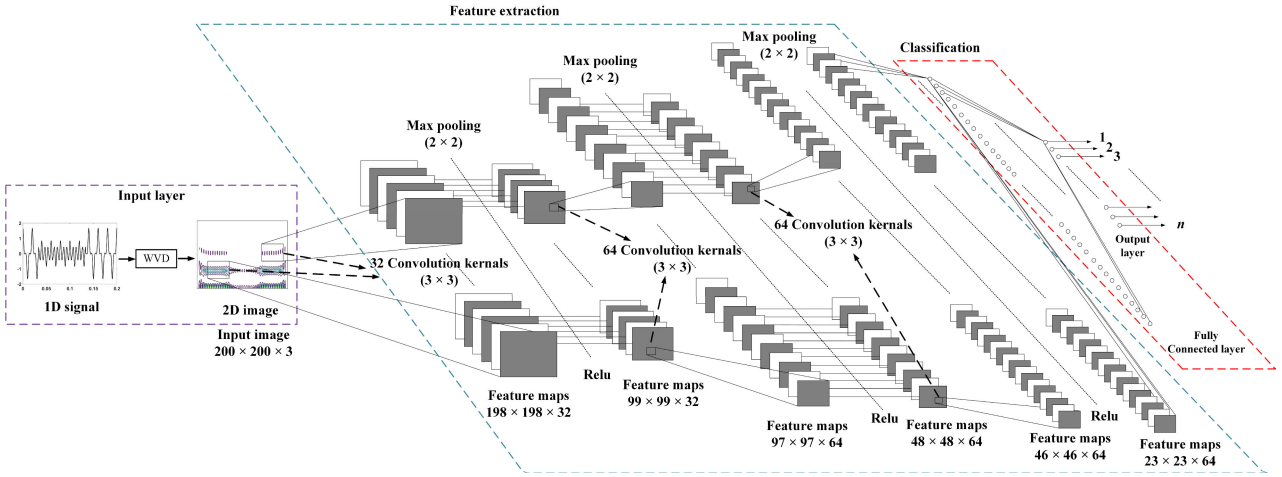

FIGURE 3. The structure of the proposed method.

the convolution operation captures the local dependencies in the image and different feature maps are generated by different kernels. Then, an activation operation is performed after every convolutional layer. It is used to introduce non-linearity in the CNN model for learning the non-linear property of the PQD data. Thereby, the rectified linear unit (ReLU) is adopted as an activation function due to its fast training speed and absence of a gradient vanishing problem. The function of ReLU is illustrated by:

$$f(x) = \max(0, x) \tag{4}$$

Then, a pooling layer is added to the ReLU function in order to reduce the dimension and number of parameters of the network. It shortens the time for the training computation and eliminates the overfitting effectively. Finally, the fully connected layer uses a softmax function to estimate the classification vector, which is then fed to the output layer.

In the proposed method, a training process is needed to tune the model. This can be carried out in five steps after all the 1D signals were transferred into 2D images:

Step 1: Initialize all the parameters of the kernels with random values.

Step 2: Divide the original images into training and testing sets. The model goes through the forward propagation step (convolutional, ReLU, max pooling and fully connected layers) and determines the output probabilities for each class with a training image. A cross-entropy function is developed as a loss function to calculate the error at the output layer:

$$e_i = -\sum_{i=1}^{n} \hat{y}_i \ln y_i \tag{5}$$

Step 3: Calculate the gradients of the error with respect to all weights and parameters in the model by using the BP technique. Then, the gradient descent is used to update all the parameter values of the kernels to minimize the output error.

Step 4: Repeat steps 2-4 with all images in the training set until the error is within the pre-set value.

Step 5: After the training process, the testing set is used to validate the accuracy of the model.

IV. RESULTS AND DISCUSSION

Here the proposed method for PQDs classification is tested by the synthetic signals established in MATLAB and real-world measurements.

A. SYNTHETIC SIGNALS

Within nine PQDs, there are 400 sample signals for each PQD, where 300 are for the training model and 100 for the test. Further, the training dataset is averagely divided into 5 sub-datasets (D1, D2, D3, D4, and D5) randomly for cross-validation. Among these subsets, one set is taken as the validation dataset, whereas other four sets are used as training data. The detailed description is shown in Table 2.

TABLE 2. The datasets of training, validation and test.

Training (240)				Validation (60)	Test (100)
D1 (60)	D2 (60)	D3 (60)	D4 (60)	D5 (60)	100
D1 (60)	D2 (60)	D3 (60)	D5 (60)	D4 (60)	100
D1 (60)	D2 (60)	D4 (60)	D5 (60)	D3 (60)	100
D1 (60)	D3 (60)	D4 (60)	D5 (60)	D2 (60)	100
D2 (60)	D3 (60)	D4 (60)	D5 (60)	D1 (60)	100

A classification model is established for training. Totally, 50 epochs are adopted in the training progress to obtain 4,391,177 optimal parameters of the model. The hardware for model training is based on an Intel (R) Core (TM) i7-6700HQ CPU @ 2.6GHz, 16GB RAM and NVIDIA GeForce GTX 970M GPU with 192-bit 3GB GDDR5 memory. The accuracy and loss curves of the training process are illustrated in Fig. 4 and the confusion matrices of

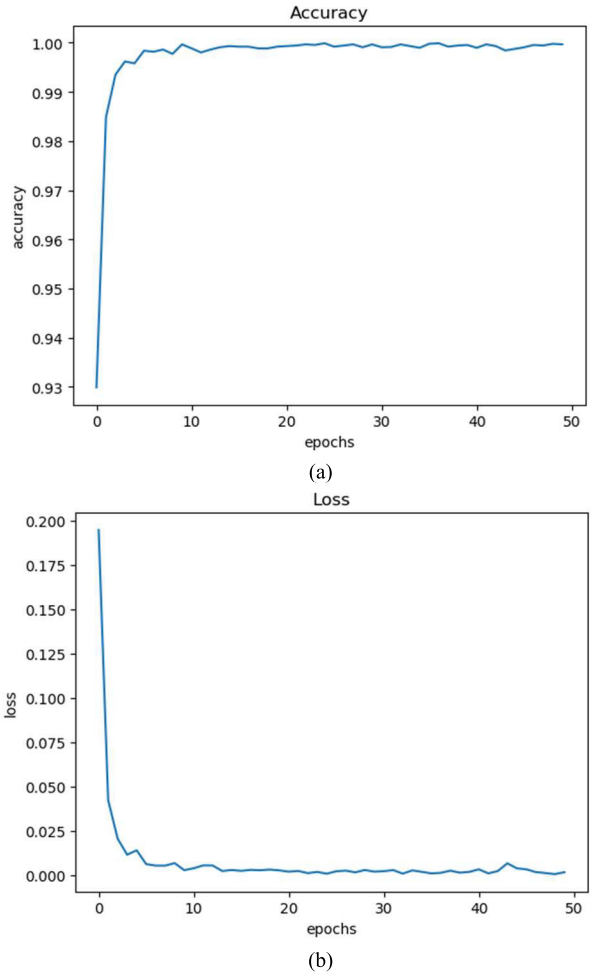

FIGURE 4. The accuracy and loss curve of the deep CNN model, (a) accuracy curve, (b) loss curve.

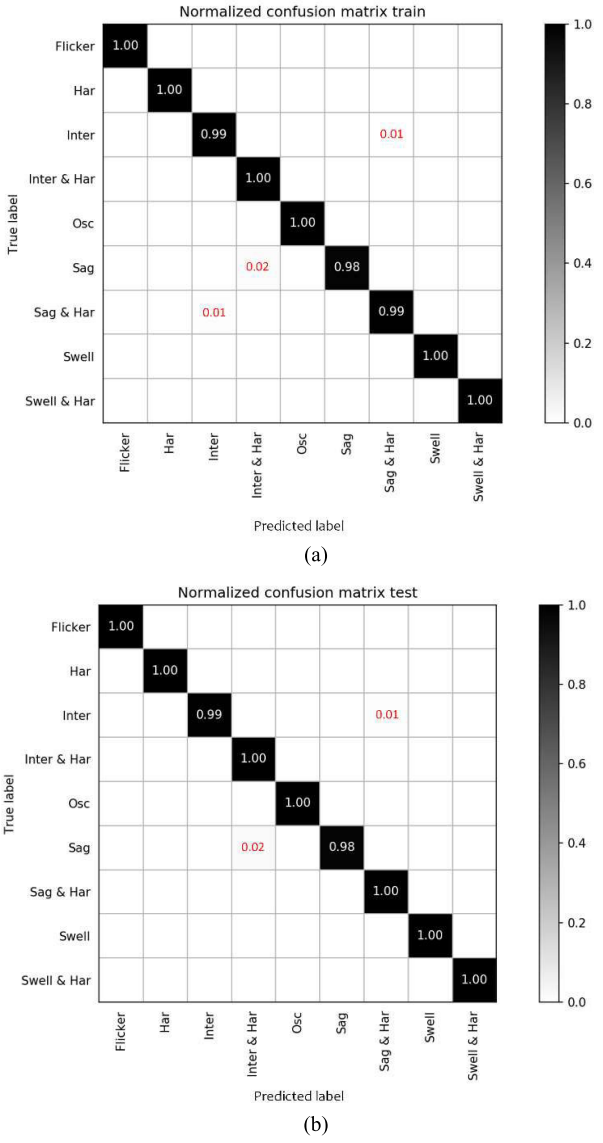

FIGURE 5. The confusion matrices of training and test results, (a) the confusion matrix of training, (b) the confusion matrix of tests.

training and test results are shown in Fig. 5. From the results, the classification accuracy of the training confusion matrix is 99.56% for both single and mixed synthetic disturbance signals. Moreover, 100 PQD events are used for testing the model, and the accuracy is 99.67%. These results have proved that the proposed WVD-CNN method can achieve a high accuracy for PQDs classification. Additionally, a comparison of the proposed PQ assessment framework with other methods is illustrated in Table 3, including five existing methods, EMD with balanced neural tree, ST with NN and DT, Hybrid ST with DT, ADALINE with FNN and VMD with DSCN. The proposed method can extract feature automatically and achieve high accuracy.

TABLE 3. The comparison of the proposed PQDs with other methods.

Method	Feature extraction (Handcrafted/Automatically)	No. of PQDs	Accuracy (%)	Ref.
EMD+Balanced Neural Tree	Hand-crafted	8	97.90	[42]
ST+NN+DT	Hand-crafted	13	99.90	[28]
Hybrid ST+DT	Hand-crafted	11	94.36	[43]
ADALINE+FNN	Hand-crafted	12	90.58	[44]
VMD+DSCN	Hand-crafted	7	99.40	[21]
WVD+CNN	Automatically	9	99.67	Proposed method

Furthermore, the output of the different convolutional layers in the deep CNN model is also demonstrated in Fig. 6. It can be seen from Fig. 6(a) that the activation of the first convolutional layer retains almost all the information present (with few blank feature maps, which are labeled with red rectangle) in the input image. In Fig. 6(b) and (c), the sparsity of the activations increases with the depth of the layer (more feature maps become blank). The features extracted from a convolutional layer become increasingly abstract and sparse with the depth of the layer. An important universal pattern of the input image is learned by the deep neural network.

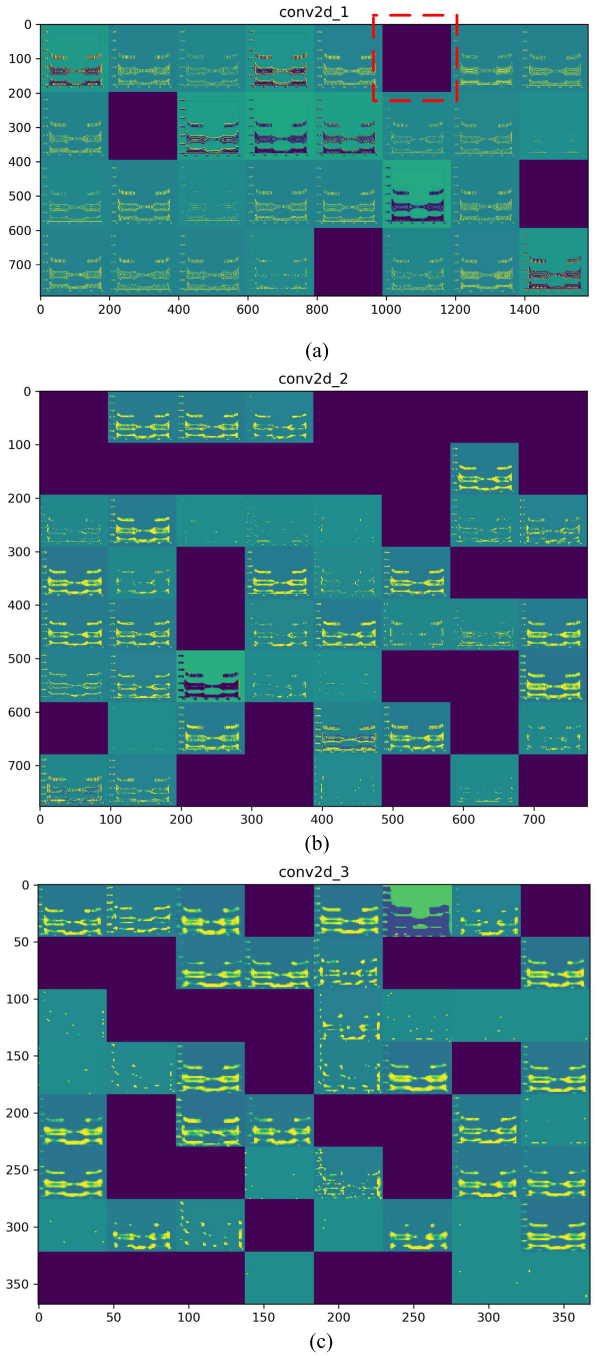

FIGURE 6. The output from different convolutional layers of the deep CNN model, (a) first layer, (b) second layer, (c) third layer.

Clearly, the deep CNN model can decrease the number of parameters of the model and simplify the structure of the model. A CNN model with 128 convolutional kernels in the third layer (other layers are the same as the proposed model) is tested in this work. The whole process is realized based on the same training principles illustrated in Section III. The model needs to be retrained with a different number of filters for comparison purposes. The output of the third layer and classification accuracy with test images are illustrated

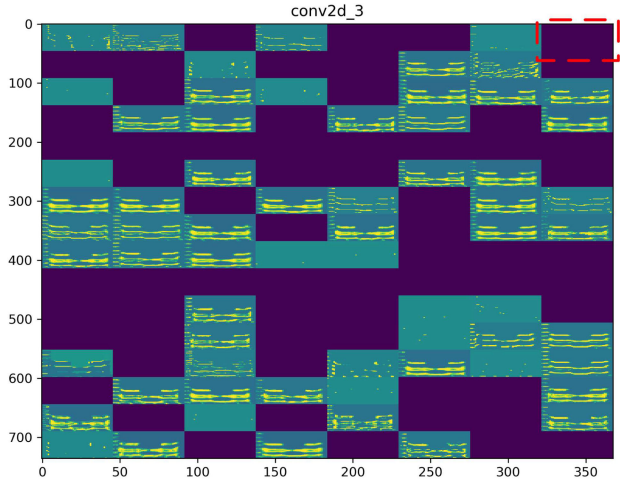

FIGURE 7. The output of the third layer with 128 convolutional kernels.

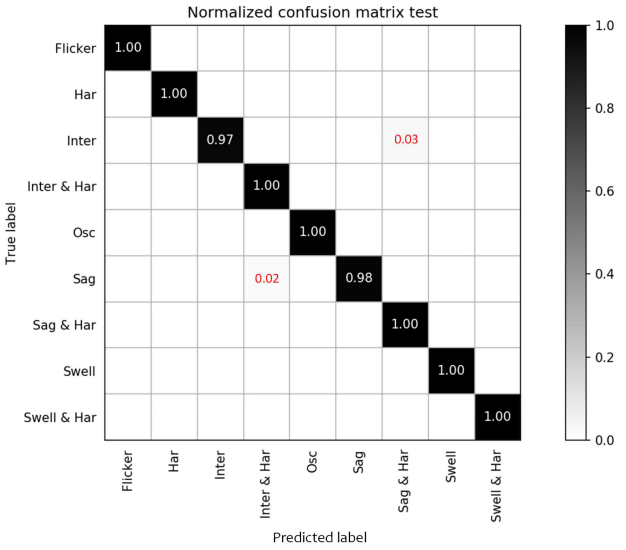

FIGURE 8. The confusion matrix of test images of the model with 128 convolutional kernels in the third layer.

in Figs. 7 and 8, respectively. In total, there are 63 blank feature maps in the third layer. This means that only half of the convolutional kernels are effective. Moreover, the number of the parameters of this model increases to 8,760,899, which is almost twice of the proposed model. The classification accuracy is 99.44% (Fig. 8), which is slightly lower than the proposed model. Thus, the proposed model is simplified and optimized through visualizing the output of different convolutional layers in the deep CNN model.

The convolutional process is to preserve the key features of the input image while eliminating insignificant ones. Hence, the blank feature maps can be obtained by convolutional operation, which is normal in the model as shown in Fig. 6. However, it would be redundant if there are too many blank blocks in the convolutional layer. It is a reason to decrease the number of kernels in the third layer rather than in the first convolutional layer for model simplification. The other reason is that the deeper the layer goes, the more

specific features the method can extract from the model, which are based on the general features extracted in the previous layer. Therefore, the key specific feature would be lost if the 32 convolutional kernels in the first layer are selected for model simplification.

Next, the effect of the incorrect classification is analyzed in this paper by a class activation map (CAM) visualization technique. The method produces a heatmap of class activation over an input image. A class activation heatmap is a 2D grid of scores associated with a specific output class, indicating the importance of each location for the class under consideration. In Fig. 5(b), there are 2 mistakes in disturbance classification: one ''interrupt'' is mistaken as a ''sag & harmonic'' disturbance; and a ''sag'' is classified as an ''interrupt & harmonic'' disturbance. The input PQD images and their heatmaps are illustrated in Figs. 9 and 10. In Fig. 9(c) and (d), there are similar hotspots located in the two figures. Hence, the classification model is misled to generate a false output obtained. Therefore, the cause of the incorrect classification can be analyzed easily through the heatmaps produced by the CAM technique.

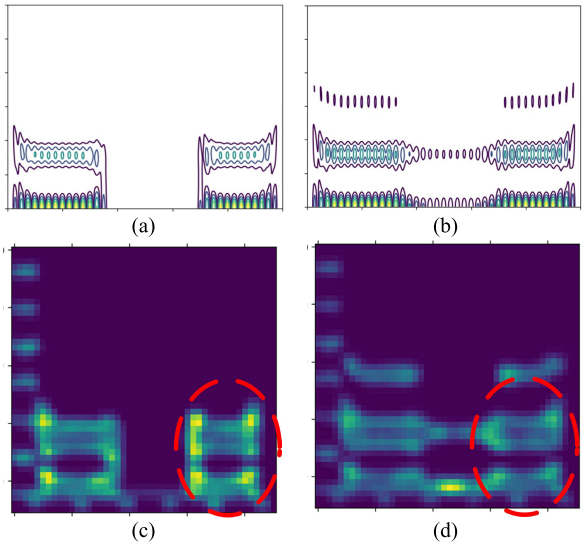

FIGURE 9. The original image and heatmap of ''interrupt'' and ''sag & harmonic'' disturbances, (a) the original image of ''interrupt'', (b) the original image of ''sag & harmonic'', (c) the heatmap of ''interrupt'', (d) the heatmap of ''sag & harmonic''.

B. REAL-WORLD MEASUREMENTS

Following the synthetic signals, three types of real-world voltage disturbance signals are from the IEEE Working Group on Power Quality Data Analytics [45]. These include flicker, swell and sag with harmonic. For each disturbance, there are 20 sampling signals, within a fundamental frequency of 60Hz and the sampling rate of 7.6kHz. The number of samples in one cycle is 128 and there are 8 cycles in every signal. The original real-world signals and their 2D images transferred by WVD are illustrated in Fig. 11. Moreover, the fundamental frequency of real-world voltage is different from the synthetic one. The frequency of WVD in (1) is 60Hz to obtain the same time-frequency domain image of the same

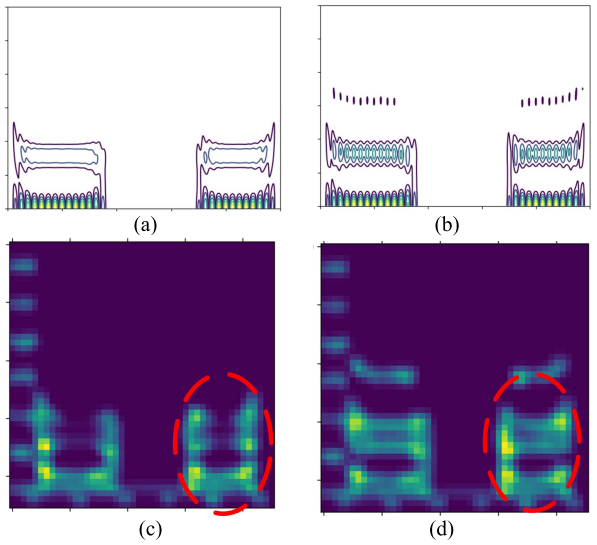

FIGURE 10. The original image and heatmap of ''sag'' and ''interrupt & harmonic'' disturbances, (a) the original image of ''sag'', (b) the original image of ''interrupt & harmonic'', (c) the heatmap of ''sag'', (d) the heatmap of ''interrupt & harmonic''.

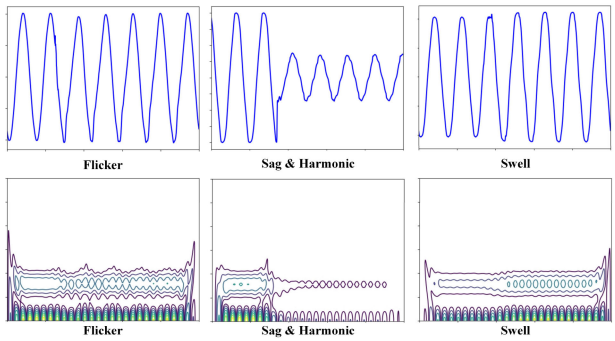

FIGURE 11. The original PQD signals and the 2D images transferred by using the WVD method.

disturbance signal. Therefore, a difference in frequency does not generate any meaningful deviations.

From Fig. 11, it can be seen that the real-world PQ disturbance signals are more complicated. Hence, several real-world signals are added to participate in the training process to fine-tune the parameters of the existing model. Then, the fine-tuned model is validated by using real-world data. From the results shown in Fig. 12, a high classification accuracy (92%) is obtained. Furthermore, the CAM technique is used to explore the cause of the lower classification accuracy. In Fig. 12, it is observed that the ''flicker'' is falsely classified to a ''swell'' disturbance. The heatmaps of the ''flicker'' and ''swell'' are produced through CAM as shown in Fig. 13. It can be seen that the original images of the two disturbances are similar to lead to a mistake.

C. DISCUSSION

From the above analysis, the PQDs can be easily classified with high accuracy by the proposed method. The feature maps can be extracted from the disturbance signals automatically

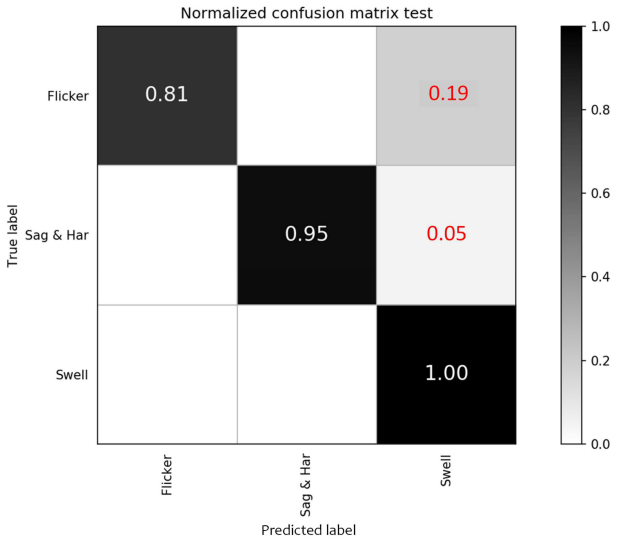

FIGURE 12. The confusion matrix of real-world signals.

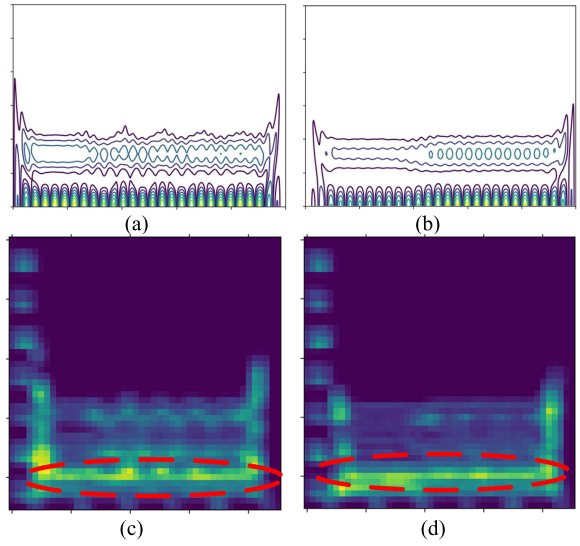

FIGURE 13. The original image and heatmap of "flicker" and "swell" disturbances, (a) the original image of "flicker", (b) the original image of "swell", (c) the heatmap of "flicker", (d) the heatmap of "swell".

without human intervention. The proposed method is excellent in the following aspects:

1) The number of the parameters and complexity of the CNN model are reduced and optimized by visualizing the feature maps of convolutional layers in the model. Specifically, the number of parameters is decreased by almost 50% from 8,760,899 to 4,391,177.

2) The CAM is introduced in this work to explore the effectiveness of PQDs classification. A heatmap is produced by this method to identify the hotspots.

3) From real-world signals, the classification accuracy can be improved by adding a small amount of real-world data into the training process to fine-tune the parameters of the model. It proves that the proposed method has excellent performance of learning and adaptation.

4) The proposed method in this paper is realized under offline conditions. However, the online implementation is also possible and is considered in future work.

V. CONCLUSION

A new algorithm based on WVD and CNN is developed for the classification of PQD signals. Firstly, the WVD method is used to transfer the 1D voltage disturbance signals into 2D images. The complicated 1D signal processing problems become simple image classification issues by the proposed method. Then, a CNN based model is established and trained through the image data to obtain optimal parameters for PQDs classification. Further, the model is simplified and optimized by visualizing the feature maps of the convolutional layers, Next, the cause of the incorrect classification is also analyzed by using the heatmaps produced by the CAM technique. The proposed method is validated and proved to achieve feature extraction and PQD classification with high accuracy.

In future work, the proposed method can be implemented online and used for multiple PQD classification, which are more challenge and practical. Finally, the PQ remedy actions can be determined according to the information provided by the proposed method.

REFERENCES

[1] P. K. Ray, S. R. Mohanty, and N. Kishor, "Classification of power quality disturbances due to environmental characteristics in distributed generation system," *IEEE Trans. Sustain. Energy*, vol. 4, no. 2, pp. 302–313, Apr. 2013.

[2] P. K. Ray, S. R. Mohanty, N. Kishor, and J. P. Catalão, "Optimal feature and decision tree-based classification of power quality disturbances in distributed generation systems," *IEEE Trans. Sustain. Energy*, vol. 5, no. 1, pp. 200–208, Jan. 2014.

[3] *Voltage Characteristics of Electricity Supplied by Public Distribution Systems*, Belgian Standard, Brussels, Belgium, 1994.

[4] *Testing and Measurement Techniques Power Quality Measurement Methods*, document IEC 61000-4-30, 2003.

[5] *IEEE Recommended Practice for Monitoring Electric Power Quality*, Standard 1159-2009, 2009.

[6] G. T. Heydt, P. S. Fjeld, C. C. Liu, D. Pierce, L. Tu, and G. Hensley, "Applications of the windowed FFT to electric power quality assessment," *IEEE Trans. Power Del.*, vol. 14, no. 4, pp. 1411–1416, Oct. 1999.

[7] Y. H. Gu and M. H. J. Bollen, "Time-frequency and time-scale domain analysis of voltage disturbances," *IEEE Trans. Power Del.*, vol. 15, no. 4, pp. 1279–1284, Oct. 2000.

[8] A. M. Gaouda, M. M. A. Salama, M. R. Sultan, and A. Y. Chikhani, "Power quality detection and classification using wavelet-multiresolution signal decomposition," *IEEE Trans. Power Del.*, vol. 14, no. 4, pp. 1469–1476, Oct. 1999.

[9] W. Gao and J. Ning, "Wavelet-based disturbance analysis for power system wide-area monitoring," *IEEE Trans. Smart Grid*, vol. 2, no. 1, pp. 121–130, Feb. 2011.

[10] P. K. Ray, N. Kishor, and S. R. Mohanty, "Islanding and power quality disturbance detection in grid-connected hybrid power system using wavelet and S-transform," *IEEE Trans. Smart Grid*, vol. 3, no. 3, pp. 1082–1094, Sep. 2012.

[11] H. H. Wang, P. Wang, and T. Liu, "Power quality disturbance classification using the S-transform and probabilistic neural network," *Energies*, vol. 10, no. 1, pp. 1–19, Jan. 2017.

[12] J. Barros, R. I. Diego, and M. Apráiz, "Applications of wavelets in electric power quality: Voltage events," *Electr. Power Syst. Res.*, vol. 88, no. 88, pp. 130–136, Jul. 2012.

[13] S. R. Mohanty, N. Kishor, P. K. Ray, and J. P. S. Catalo, "Comparative study of advanced signal processing techniques for islanding detection in a hybrid distributed generation system," *IEEE Trans. Sustain. Energy*, vol. 6, no. 1, pp. 122–131, Jan. 2015.
[14] V. Climente-Alarcon, J. A. Antonino-Daviu, A. Haavisto, A. Arkkio, "Diagnosis of induction motors under varying speed operation by principal slot harmonic tracking," *IEEE Trans. Ind. Appl.*, vol. 51, no. 5, pp. 3591–3599, Sep./Oct. 2015.
[15] S. Shukla, S. Mishra, and B. Singh, "Empirical-mode decomposition with Hilbert transform for power-quality assessment," *IEEE Trans. Power Del.*, vol. 24, no. 4, pp. 2159–2165, Oct. 2009.
[16] A. H. Mohammad and S. Afsharnia, "A new passive islanding detection method and its performance evaluation for multi-DG systems," *Electr. Power Syst. Res.*, vol. 110, pp. 180–187, May 2014.
[17] N. E. Huang, Z. Shen, S. R. Long, M. C. Wu, H. H. Shih, Q. Zheng, N.-C. Yen, C. C. Tung, and H. H. Liu, "The empirical mode decomposition and the Hilbert spectrum for nonlinear and non-stationary time series analysis," *Proc. Roy. Soc. London. A, Math., Phys. Eng. Sci.*, vol. 454, no. 1971, pp. 903–995, Mar. 1998.
[18] K. Cai, Z. Wang, G. Li, D. He, and J. Song, "Harmonic separation from grid voltage using ensemble empirical-mode decomposition and independent component analysis," *Int. Trans. Electr. Energy*, vol. 27, no. 2, Nov. 2017, Art. no. e2405.
[19] K. Dragomiretskiy and D. Zosso, "Variational mode decomposition," *IEEE Trans. Signal Process.*, vol. 62, no. 3, pp. 531–544, Feb. 2014.
[20] P. D. Achlerkar, S. R. Samantaray, and M. S. Manikandan, "Variational mode decomposition and decision tree based detection and classification of power quality disturbances in grid-connected distributed generation system," *IEEE Trans. Smart Grid*, vol. 9, no. 4, pp. 3122–3132, Jul. 2018.
[21] K. Cai, B. P. Alalibo, W. Cao, Z. Liu, Z. Wang, and G. Li, "Hybrid approach for detecting and classifying power quality disturbances based on the variational mode decomposition and deep stochastic configuration network," *Energies*, vol. 11, no. 11, p. 3040, Nov. 2018.
[22] Z. Li, J. Chen, Y. Zi, and J. Pan, "Independence-oriented VMD to identify fault feature for wheel set bearing fault diagnosis of high speed locomotive," *Mech. Syst. Signal Process*, vol. 85, pp. 512–529, Feb. 2017.
[23] C. Yi, Y. Lv, and Z. Dang, "A fault diagnosis scheme for rolling bearing based on particle swarm optimization in variational mode decomposition," *Shock Vib*, May 2016, Art. no. 9372691.
[24] Z. Liu, Y. Cui, and W. Li, "A classification method for complex power quality disturbances using EEMD and rank wavelet SVM," *IEEE Trans. Smart Grid*, vol. 6, no. 4, pp. 1678–1685, Jul. 2015.
[25] J. Li, Z. Teng, Q. Tang, and J. Song, "Detection and classification of power quality disturbances using double resolution S-transform and DAG-SVMs," *IEEE Trans. Instrum. Meas.*, vol. 65, no. 10, pp. 2302–2312, Oct. 2016.
[26] M. Biswal and P. K. Dash, "Measurement and classification of simultaneous power signal patterns with an S-transform variant and fuzzy decision tree," *IEEE Trans Ind. Informat.*, vol. 9, no. 4, pp. 1819–1827, Nov. 2013.
[27] F. A. S. Borges, R. A. S. Fernandes, I. N. Silva, and C. B. S. Silva, "Feature extraction and power quality disturbances classification using smart meters signals," *IEEE Trans. Ind. Informat.*, vol. 12, no. 2, pp. 824–833, Apr. 2016.
[28] R. Kumar, B. Singh, D. T. Shahani, A. Chandra, and K. Al-Haddad, "Recognition of power-quality disturbances using S-transform-based ANN classifier and rule-based decision tree," *IEEE Trans. Ind. Appl.*, vol. 51, no. 2, pp. 1249–1258, Mar./Apr. 2015.
[29] K. Manimala and K. Selvi, "Power disturbances classification using S-transform based GA–PNN," *J. Inst. Eng.*, vol. 96, no. 3, pp. 283–295, Sep. 2015.
[30] K. M. Silva, B. A. Souza, and N. S. D. Brito, "Fault detection and classification in transmission lines based on wavelet transform and ANN," *IEEE Trans. Power Del.*, vol. 21, no. 4, pp. 2058–2063, Oct. 2006.
[31] G. O. Young, "Historical trends in deep learning," in *Deep Learning*, vol. 3, 1st ed. Cambridge, MA, USA: MIT, 2016, pp. 11–28.
[32] D. Zhang, X. Han, and C. Deng, "Review on the research and practice of deep learning and reinforcement learning in smart grids," *CSEE J. Power Energy Syst.*, vol. 4, no. 3, pp. 362–370, Sep. 2018.
[33] M. Matsugu, K. Mori, Y. Mitari, and Y. Kaneda, "Subject independent facial expression recognition with robust face detection using a convolutional neural network," *Neural Netw.*, vol. 16, nos. 5–6, pp. 555–559, Jul. 2003.
[34] M. Baccouche, F. Mamalet, C. Wolf, C. Garcia, and A. Baskurt. *Sequential Deep Learning for Human Action Recognition*. Berlin, Germany: Springer, 2011, pp. 29–39.
[35] H. A. Malki and A. Moghaddamjoo, "Using the Karhunen-Loe've transformation in the back-propagation training algorithm," *IEEE Trans. Neural Netw.*, vol. 2, no. 1, pp. 162–165, Jan. 1991.
[36] H. Liao, J. V. Milanovic, M. Rodrigues, and A. Shenfield, "Voltage sag estimation in sparsely monitored power systems based on deep learning and system area mapping," *IEEE Trans. Power Del.*, vol. 33, no. 6, pp. 3162–3172, Dec. 2018.
[37] N. Mohan, K. P. Soman, and R. Vinayakumar, "Deep power: Deep learning architectures for power quality disturbances classification," in *Proc. TAP Energy*, Dec. 2017, pp. 1–6.
[38] C.-M. Li, Z.-X. Li, N. Jia, Z.-J. Qi, and J.-H. Wu, "Classification of power-quality disturbances using deep belief network," in *Proc. ICWAPR*, Jul. 2018, pp. 231–237.
[39] Z. Qin, F. Yu, C. Liu, and X. Chen, "How convolutional neural network see the world - A survey of convolutional neural network visualization methods," Apr. 2018, *arXiv:1804.11191*. [Online]. Available: https://arxiv.org/abs/1804.11191
[40] J. Yosinski, J. Clune, A. Nguyen, T. Fuchs, and H. Lipson, "Understanding neural networks through deep visualization," *Comput. Sci.*, Jun. 2015. [Online]. Available: https://arxiv.org/abs/1506.06579
[41] S. Lawrence, C. L. Giles, A. C. Tsoi, and A. D. Back, "Face recognition: A convolutional neural-network approach," *IEEE Trans. Neural Networ.*, vol. 8, no. 1, pp. 98–113, Jan. 2012.
[42] B. Biswal, M. Biswal, S. Mishra, and R. Jalaja, "Automatic classification of power quality events using balanced neural tree," *IEEE Trans. Ind. Electron.*, vol. 61, no. 1, pp. 521–530, Jan. 2014.
[43] M. Biswal and P. K. Dash, "Detection and characterization of multiple power quality disturbances with a fast S-transform and decision tree based classifier," *J. Digit. Signal Process.*, vol. 23, no. 4, pp. 1071–1083, Jul. 2013.
[44] M. Valtierra-Rodriguez, R. de Jesus Romero-Troncoso, R. A. Osornio-Rios, and A. Garcia-Perez, "Detection and classification of single and combined power quality disturbances using neural networks," *IEEE Trans. Ind. Electron.*, vol. 61, no. 5, pp. 2473–2482, May 2014.
[45] W. Freitas, T. A. Cooke, and K. Kittredge. *IEEE Working Group on Power Quality Data Analytics*. Accessed: Apr. 2019. [Online]. Available: http://grouper.ieee.org/groups/td/pq/data/

KEWEI CAI received the B.S. and Ph.D. degrees from the School of Electrical Engineering, Dalian University of Technology (DLUT), Dalian, China, in 2007 and 2014, respectively.

He was a Visiting Scholar with Aston University, U.K., from September 2018 to August 2019. He is currently a Lecturer with Dalian Ocean University (DLOU). His current research interests include artificial intelligence technic in power systems, power electronics, wind power generation, and electrified vehicles.

WENPING CAO (M'05–SM'11) received the B.Eng. degree in electrical engineering from Beijing Jiaotong University, Beijing, China, in 1991, and the Ph.D. degree in electrical machines and drives from the University of Nottingham, Nottingham, U.K., in 2004. He is currently a Chair Professor of electrical power engineering with Aston University, Birmingham, U.K., and a Visiting Professor with the College of Electrical and Power Engineering, Taiyuan University of Technology, China.

LASSI AARNIOVUORI (M'14) was born in Jyväskylä, Finland, in 1979. He received the M.Sc. degree in electrical engineering and the D.Sc. degree in electric motors and drives from the Lappeenranta University of Technology (LUT), Lappeenranta, Finland, in 2005 and 2010, respectively.

He was a Marie Curie Fellow with the School of Engineering and Applied Science, Aston University, Birmingham, U.K. He is currently an Adjunct Professor with the LUT School of Energy Systems, LUT University. His current research interests include the field of electric motors and drives, especially wide band-gap power switches, modulation methods, simulation of electric drives, efficiency measurements, and calorimetric measurement systems.

HONGSHUAI PANG was born in Dalian, Liaoning, China, in 1982. He received the B.S. degree in electrical engineering from the Shenyang University of Technology (SUT), in 2005, and the M.S. degree in traffic information engineering and control from Dalian Jiaotong University, in 2009.

Since 2009, he has been a Lecturer with the Information Engineering Department, Dalian Ocean University. He is currently an Associate Editor of four books and more than 20 research projects. His current research interests include marine information technology, artificial intelligence technology, and the IoT Technology.

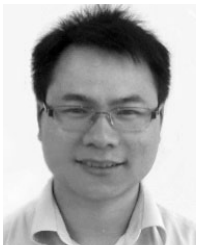

YUANSHAN LIN received the M.S. and Ph.D. degrees from the School of Computer Science, Dalian University of Technology (DLUT), Dalian, China, in 2008, and 2013, respectively.

He is currently an Associate Professor with the School of Information Science and Engineering, Dalian Ocean University (DLOU). His current research interests include robotics and control, in particular, robot learning, motion planning, automatous navigation, and machine learning.

GUOFENG LI received the Ph.D. degree from the Dalian University of Technology (DLUT), Dalian, China, in 2000, where he is currently a Professor and the Dean of the School of Electrical Engineering.

His current research interests include electric machines and drives, power electronics, wind power generation, electrified vehicles, measurement techniques, and power system analysis.